

## Direct Observation of a Pressure-Induced Precursor Lattice in Silicon

Guoyin Shen,<sup>1,\*</sup> Daijo Ikuta,<sup>1</sup> Stanislav Sinogeikin,<sup>1</sup> Quan Li,<sup>2,3</sup> Yi Zhang,<sup>2</sup> and Changfeng Chen<sup>2</sup>

<sup>1</sup>*High Pressure Collaborative Access Team, Geophysical Laboratory, Carnegie Institution of Washington, Argonne, Illinois 60439, USA*

<sup>2</sup>*Department of Physics and High Pressure Science and Engineering Center, University of Nevada, Las Vegas, Nevada 89514, USA*

<sup>3</sup>*College of Materials Science and Engineering, State Key Laboratory of Superhard Materials, Jilin University, Changchun 130012, China*

(Received 14 June 2012; published 16 November 2012)

Detailed knowledge of atomic-scale structural change is essential for understanding the process and mechanism of phase transitions in solids. We present the direct experimental evidence of a precursor lattice in silicon at high pressures. The precursor lattice may appear to coexist dynamically with the host lattice over a large pressure range through rapid lattice fluctuations. The first-principles calculations are used to elucidate a dynamic lattice-fluctuation mechanism that accounts for the experimental observations. This precursor lattice-fluctuation mechanism for the phase transition goes beyond previously considered reconstructive or displacive processes and provides a novel picture of the underlying dynamics.

DOI: [10.1103/PhysRevLett.109.205503](https://doi.org/10.1103/PhysRevLett.109.205503)

PACS numbers: 81.40.Vw, 07.35.+k, 61.05.cp, 61.50.Ks

Silicon displays a phase transition from the tetrahedrally coordinated cubic diamond structure ( $\alpha$  phase) to the octahedrally coordinated tetragonal  $\beta$ -Sn structure ( $\beta$  phase) at around 13 GPa [1–3] accompanied by a large volume collapse of about 22% [2,4] and an abrupt electric resistivity decrease of more than 5 orders of magnitude [1]. The  $\alpha$ - $\beta$  phase transition in silicon has long been considered a prototypical strongly first-order transition with no indication of precursors. In this Letter, we report direct experimental observations of the electron density distributions for a silicon single crystal at high pressures, revealing two closely correlated active groups of silicon atoms that develop progressively with increasing pressure and exhibit a strong enhancement at pressures close to the  $\alpha$ - $\beta$  phase transition. Our combined experimental and theoretical analysis indicates a novel dynamic mechanism which shows that the high-pressure  $\beta$  phase can dynamically coexist with the host lattice of the low-pressure  $\alpha$  phase through rapid lattice fluctuations. These results provide insights for understanding the origin and mechanism of the  $\alpha$ - $\beta$  phase transition.

A silicon wafer in single crystal form ([5]) was loaded into a diamond anvil cell (DAC) with rhenium as gasket material and helium as pressure transmitting medium. The wafer had dimensions of  $45 \times 35 \mu\text{m}^2$  with a thickness of  $25 \mu\text{m}$ . Our experiments were performed at the 16-BM-D station at HPCAT at the Advanced Photon Source [6]. We deduce electron density distributions from structure factor measurements and resolve crystal structures at high pressures with unprecedented accuracy using the recently developed single crystal x-ray diffraction (SCXRD) technique. A DAC with a large opening ( $70^\circ$ ) was used for a large coverage in reciprocal space. We have developed a data collecting procedure that reliably measures diffraction intensities, through which

we have obtained crystallographic information of space groups, atomic positions, and thermal parameters as a function of pressure up to 13.1 GPa, the highest pressure before the single crystal was broken due to the  $\alpha$ - $\beta$  phase transition. The difference Fourier method and the maximum entropy method [7] were used to obtain the electron density maps from the structural factors of (hkl) orientations. The details of the experimental procedures and the data analysis are presented in the Supplemental Material [8]. The obtained  $R$  factors (see Table s1 [8]) indicate good quality of the SCXRD data from the high pressure sample.

Figure 1 shows the electron density distributions for silicon measured at high pressures. At the lowest pressure of 1.4 GPa in this study, the electron density distribution clearly represents the cubic diamond structure of the  $\alpha$ -Si phase [Figs. 1(a) and 1(b)]. At increased pressure, we observed pressure-induced changes in electron density distributions that are signified by two active groups, as seen in Figs. 1(c) and 1(d) where data at 12.4 GPa are shown. One active group [shown in green in Figs. 1(c) and 1(d)] consists of six positions surrounding each silicon atom in the diamond structure; it is referred to as the vicinity group hereafter. Compared to the silicon position of  $(1/8, 1/8, 1/8)$  in the host lattice, the six atomic positions of the vicinity group can be expressed by  $(1/8 \pm \Delta, 1/8, 1/8)$ ,  $(1/8, 1/8 \pm \Delta, 1/8)$ ,  $(1/8, 1/8, 1/8 \pm \Delta)$  on the  $48f$  Wyckoff sites of the  $Fd\bar{3}m$  space group. The displacement distance,  $\Delta$ , changes only slightly with pressure, from a value of 0.22 at  $\sim 3$  GPa to 0.18 at 12.4 GPa. The shape of the electron density distribution is nearly identical at these positions, appearing like an inflated pentagon, as shown in Fig. 1(e). The orientation of these pentagons is not random, but a  $90^\circ$  rotation relative to the position at the other side of a

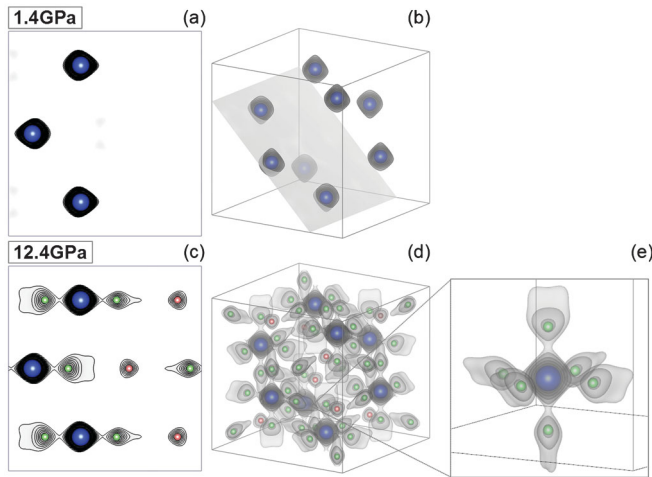


FIG. 1 (color). Electron density distributions in silicon at high pressures. (a) and (b) the electron density maps at 1.4 GPa, where (a) is a slide image along the [110] plane as indicated in (b). The electron density data reveal a lattice in diamond structure at 1.4 GPa. (c) and (d) the electron density data at 12.4 GPa where the two active groups are clearly observed; (c) a slide image along the [110] plane as in (a). The host lattice of the  $\alpha$  phase is represented by the symbols in blue. The void group is shown in red, while the vicinity group in green. The local distribution of the vicinity group has the point-group symmetry of  $S_4$  as shown in (e).

silicon atom, resulting in a local symmetry of the vicinity group being the point group of  $S_4$ .

The second active group is situated in the “void” sites of the open diamond structure. In the tetrahedral environment of the host lattice, each silicon atom has a void site aligned opposite to one of its nearest-neighbor atoms [Fig. 1(b)]. The void positions and silicon positions of the host lattice can be viewed as two sublattices separated by  $\frac{1}{2}$  along a crystallographic axis. Under compression, our electron density maps show that these void positions are populated by silicon atoms [shown in red in Figs. 1(c) and 1(d)], forming the second active group (called the void group hereafter). The lattice position of the void group is at  $(1/8, 1/8, 1/8 + 1/2)$  ( $8b$  Wyckoff sites).

From the electron density distributions, we can get information on the occupancies of the active groups via integration in a volume centered on each active group site. Figure 2 shows the occupation factors of the active groups relative to those of the host lattice as a function of pressure. It is seen that the occupation factors of the two active groups are closely correlated, showing a maximum at around 12.2–12.4 GPa. The vicinity group can be first recognized at 2.6 GPa, and its occupation factor increases with increasing pressure. Starting at about 10.5 GPa, there is a strong enhancement in the occupation factor until 12.4 GPa, above which an appearance of the  $\beta$  phase was observed (see Fig. s2 in the Supplemental Material [8]), while the host crystal still displays its single crystal nature in the diamond structure. The appearance of the  $\beta$  phase

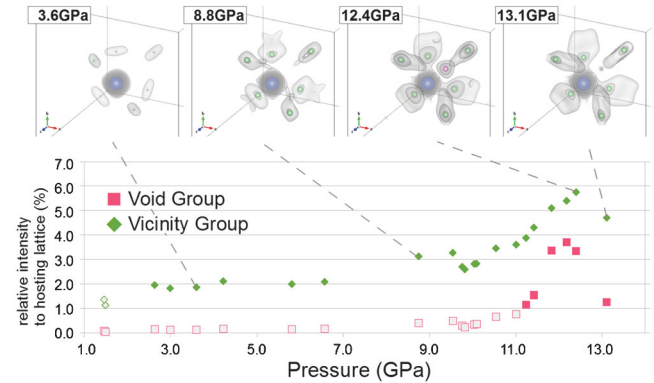


FIG. 2 (color). Integrated intensities of the two active groups relative to those of the host lattice as a function of pressure (bottom). The intensities of the active groups are obtained by integrating charge densities in a volume surrounding each active group site. The local electron density maps are shown at four different pressure points as indicated in the top. The solid symbols in the intensity plot represent the data where active groups are formed and clearly visible, while open symbols represent scattered intensities from the same volumes of the vicinity or void sites where the active groups are not clearly identified.

comes at a cost of the  $\alpha$  phase, causing the decrease of the occupation factor of active groups at 13.1 GPa (Fig. 2). The first recognizable appearance of the void group is at 11.2. Similar to the case for the vicinity group, the occupation factor of the void group peaks at 12.2 GPa and then drops at higher pressures. The overall occupation factors of the vicinity group are roughly 2% higher than those of the void group, but they are otherwise similar in trends to each other, following the same trend with increasing pressure. Similar occupancies of the two active groups can be also estimated by putting silicon atoms at both the void and vicinity positions of the  $Fd-3m$  space group and refining their occupancies with the constraint that the total number of silicon atoms is constant (see Table s2 in the Supplemental Material [8]). This close correlation of the occupation factors of the two active groups as a function of pressure suggests that they manifest the same collective phenomenon and are of the same origin. The earlier appearance and higher occupation factor of the vicinity group can be understood by considering the effect of the atomic vibrations in the  $\alpha$  phase, which have fairly large amplitudes due to the strong anharmonicity and lattice softening with increasing pressure (see Supplemental Material [8]). These vibrations can move silicon atoms into the space surrounding the vicinity group sites, thus contributing to the occupation factor. Meanwhile, the void group positions are too far away from the atomic sites in the  $\alpha$  phase to be populated via such a vibration-driven process. We will show below that the increasingly favorable energetic and kinetic environment at higher pressures introduces a new dynamic mechanism that drives silicon atoms toward both the vicinity and void group sites, which

explains their parallel rise approaching the transition pressure.

A major clue to resolving the puzzle of the structural relation between the active groups and the host lattice comes from the fact that the lattice positions of the two active groups are directly related to the atomic positions of the  $\beta$ -Sn structure. Figure 3 demonstrates the relationship of the active groups to the tetragonal  $\beta$ -Sn lattice, and the latter can be constructed from the positions of the two active groups as indicated in Fig. 3(b). Because each six-member positions of the vicinity group [Fig. 1(e)] can be considered as one equivalent atomic position averaged at the silicon position in the host lattice, the unit cell of the  $\beta$ -Sn structure in Fig. 3(b) is constructed from the combination of the void positions and silicon positions of the host lattice. The tetragonal symmetry of the  $\beta$ -Sn structure comes from the atomic displacement ( $\Delta$ ) of the vicinity group; it gives a stretching along the [100] and [010] directions, and the resulting lattice displays the tetragonal symmetry of the  $\beta$ -Sn structure. Therefore, the two active groups behave as a precursor of the  $\beta$ -Sn lattice in the host lattice. The increased occupancy of the void sites in  $\alpha$  phase eventually results in the  $\alpha$ - $\beta$  transition (Fig. 2). The void site occupation may be also responsible for the low-density to high-density transition in amorphous silicon [9,10], where the transition is accompanied by increased occupancy of the void sites, resulting in an increase in the mean coordination number to 4.6 [11].

To distinguish whether the pressure-induced precursor exists in nucleated static domains scattered in the host lattice or in fast dynamic lattice fluctuations, we have performed a separate experiment with a single crystal of silicon in a helium medium with a DAC. The pressure was first increased to 11.8 GPa, where again we clearly

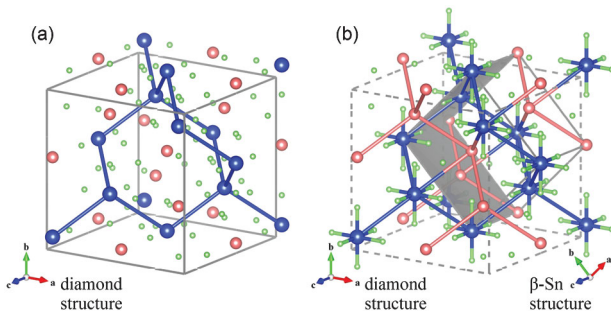


FIG. 3 (color). (a) Atomic positions of the host diamond structure (blue) together with the two active groups (red: the void group, green: the vicinity group). A unit cell of the diamond structure is shown by connecting the blue atomic positions. (b) A new unit cell by combining the void group (red sublattice) with the vicinity group (blue sublattice which represents the averaged equivalent positions of the vicinity group). The unit cell orientation is shown in the lower-right corner of (b). The tetragonal symmetry of the  $\beta$ -Sn structure originates from the atomic displacements of the vicinity group which gives a stretching along the [100] and [010] directions.

observed two active groups consistent with those shown in Figs. 1 and 2. After the SCXRD measurement, the pressure increased slightly to a value of 12.2 GPa. Instead of further increasing pressure, which would lead to an irreversible  $\alpha$ - $\beta$  phase transition and the breakage of the single crystal, we released pressure to look for possible signs of remnants of the nucleated  $\beta$  phase, which is known to exist in a metastable form and not return to the starting lattice structure of the  $\alpha$  phase upon decompression [2,4]. Our experiment showed, however, that the active groups faded away after pressure was released, leaving a host lattice that is the same as the starting material with no signs of any secondary phase. These results suggest that the precursor in silicon at high pressures appear dynamically through fast lattice fluctuations.

We have performed first-principles calculations (see the Supplemental Material [8] for details) to understand the energetic and kinetic aspects associated with the pressure-induced  $\alpha$ - $\beta$  phase transition of silicon. We show in Fig. 4 the calculated enthalpy change (relative to that of the  $\alpha$

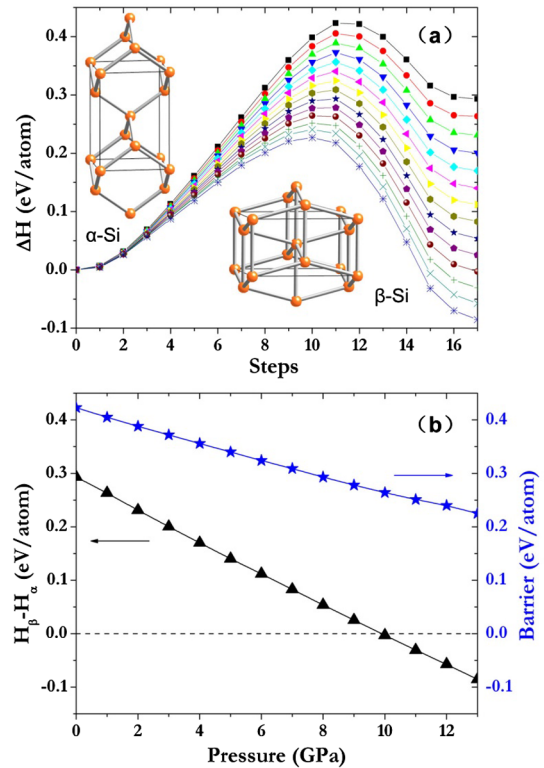


FIG. 4 (color online). (a) The calculated enthalpy change,  $\Delta H$ , relative to the value for  $\alpha$ -Si along the pathway for the phase transformation, which proceeds with a continual reduction of the  $c/a$  ratio over the pressure range of 0 to 13 GPa (top to bottom curves at a pressure step of 1 GPa). The two structures ( $\alpha$ -Si and  $\beta$ -Si) are depicted in a common body-centered-tetragonal cell to show the change and relation of the atomic positions in the two structures. (b) The enthalpy difference between  $\beta$ -Si and  $\alpha$ -Si,  $H_{\beta} - H_{\alpha}$ , and the kinetic barrier as a function of pressure extracted from the first-principles results shown in (a).

phase) along the transformation pathway toward the  $\beta$  phase over a pressure range of 0 to 13 GPa. It is seen that the  $\beta$  phase has its enthalpy reduced monotonically with increasing pressure and becomes energetically more favorable above the thermal equilibrium pressure  $P_t$  at 9.90 GPa, which agrees well with previously calculated data [12,13]. Moreover, the kinetics also becomes more favorable with the enthalpy barrier for the  $\alpha$ - $\beta$  transition decreasing significantly (from 0.423 eV/atom at 0 GPa to 0.264 eV/atom at 10 GPa) with rising pressure. This produces an energetic and kinetic landscape conducive to dynamic phase fluctuations between the  $\alpha$  and  $\beta$ -Si lattices. These results demonstrate that high pressure produces an increasingly favorable energetic and kinetic environment for silicon atoms to move about and explore the phase space, making it possible for the transient (i.e., dynamic) occupation of the vicinity and void group sites prior to the  $\alpha$ - $\beta$  phase transition.

The energetic results from first-principles calculations allow a quantitative evaluation of the occupation factor of the active groups compared to that of the host lattice based on thermodynamic considerations (see the Supplemental Material [8] for details). To quantitatively compare the calculated results with the experimental data, we present the relative intensities as a function of reduced pressure  $P/P_t$  in Fig. 5. We used the same set of enthalpy-versus-pressure data extracted from the results in Fig. 4 for both active groups, except for a constant (2%) positive offset for the vicinity group to account for the contributions from the thermal vibrations as discussed above. The excellent agreement between the theoretical and experimental data provides compelling evidence supporting the dynamic phase fluctuation mechanism for the appearance of the precursor lattice in silicon under pressure.

It is known that the structural phase transition of silicon is accompanied by a semiconductor-metal transition [14]. We have performed band-structure calculations (see the Supplemental Material [8] for details) to study the relation between the precursor lattice and the electronic transition, and found that the appearance of a relatively small amount of void and vicinity precursors near the transition pressure effectively reduces the band gap of silicon, leading to the semiconductor-metal transition. This result is suggestive of a broader influence of the pressure-induced precursor in the conduction and other properties of the silicon material. Further studies on “property-precursor” relations are needed for insights in establishing predictive models.

The “forbidden” (222) reflection has long been used for studying the anticosymmetric charge density and anharmonicity of silicon lattice [15–17]. Using x-ray diffraction, the intensities of the forbidden (222) reflection at high pressures [17] displayed a sudden increase at around 11 GPa and then decreased above  $\sim 12$  GPa. The behavior of the (222) reflection intensity as a function of pressure is similar to those of the two active groups as shown in Fig. 2,

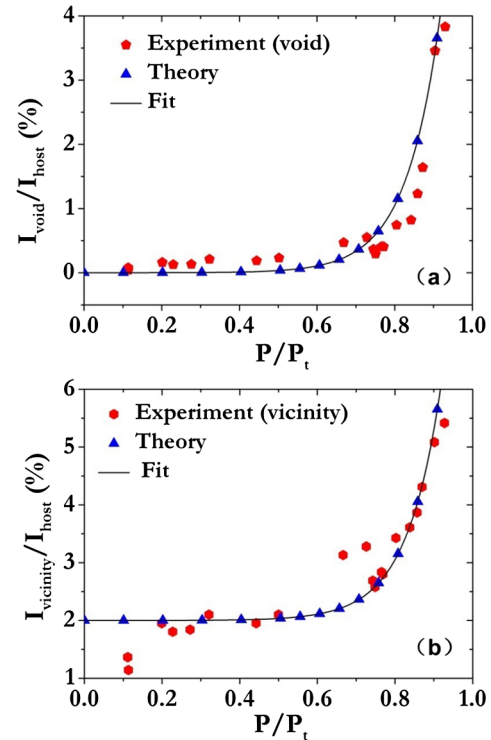


FIG. 5 (color online). The theoretical values compared to the experimental data for the relative intensities of (a) the void group and (b) the vicinity group as a function of reduced pressure  $P/P_t$ . The theoretical values in the fit are obtained using the first-principles energetic results shown in Fig. 4 (see the Supplemental Material [8] for details).

which implies that the (222) reflection intensity may be used as a measure of the degree of the precursor. The sharp decrease in the (222) intensity [17] can then be understood as a result of the appearance of the  $\beta$  phase.

Although precursor phenomena have been observed in several metallic alloys and oxides [18–22] driven by temperature, particularly in connection with martensitic transformations and incomplete lattice instability, the precursor in silicon observed in the present work contrasts sharply in several ways: (i) it is observed in a simple elemental solid; (ii) it is related to a strongly first-order phase transition; and (iii) it is driven by pressure, which greatly broadens our experimental capability and overall understanding of the lattice instability from the dynamic fluctuation point of view. The finding of the pressure-induced active groups in silicon suggests a new paradigm for understanding precursor phenomena in phase transitions, which has broad implications for a large class of materials that need to be reexamined by the latest high-accuracy experimental techniques for the possible presence of precursors.

In summary, our combined experimental and theoretical analysis indicates a novel dynamic mechanism which shows that the high-pressure  $\beta$  phase can dynamically coexist with the host lattice of the low-pressure  $\alpha$  phase through rapid lattice fluctuations. At pressures close to the

phase transition, the precursor components increase exponentially (Figs. 2 and 5) until they reach a threshold level at 7%–8% (Fig. 2). Beyond this threshold, the host lattice can no longer persist as the dominant lattice in the fluctuation process and eventually collapses. This precursor lattice-fluctuation mechanism for the  $\alpha$ - $\beta$  phase transition goes beyond previously considered reconstructive or displacive processes [23] and provides a deeper understanding of the underlying dynamics. Fast phase fluctuations have been reported in other materials at high pressures [24] to interpret the experimentally observed coexistence of two phases. Our present work, however, provides the quantitative description of the embryonic lattice (precursor) in the host lattice via an accurate three-dimensional mapping. These results provide insights for understanding the origin and mechanism of the  $\alpha$ - $\beta$  phase transition. This new capability to explore precursor phenomena in phase transitions may greatly expand our knowledge of atomic-scale processes related to structural phase transitions at high pressure.

We thank M. Somayazulu and M. Guthrie for their comments, W. Yang for providing the silicon sample, and S. Tkachev for the help in using the gas-loading system which is supported by GSECARS and COMPRES. This work was partly supported by EFree, an Energy Frontier Research Center funded by the U.S. Department of Energy (No. DESC0001057). Work at UNLV was supported by DOE under Cooperative Agreement DE-FC52-06NA26274. HPCAT operations are supported by CIW, CDAC, UNLV, and LLNL through funding from DOE-NNSA and DOE-BES, with partial instrumentation funding by NSF. The Advanced Photon Source is supported by DOE-BES, under Contract No. DE-AC02-06CH11357.

---

\*Corresponding author.  
gshen@ciw.edu

- [1] S. Minomura and H. G. Drickamer, *J. Phys. Chem. Solids* **23**, 451 (1962).  
 [2] J. Z. Hu and I. L. Spain, *Solid State Commun.* **51**, 263 (1984).  
 [3] B. A. Weinstein and G. J. Piermarini, *Phys. Rev. B* **12**, 1172 (1975).  
 [4] J. C. Jamieson, *Science* **139**, 762 (1963).  
 [5] See <http://universitywafer.com>.  
 [6] G. Shen *et al.*, *High Press. Res.* **28**, 145 (2008).  
 [7] F. Izumi and R. A. Dilanian, *Recent Research Developments in Physics* (Transworld Research Network, Trivandrum, 2002), Vol. 3, Part II, p. 699.  
 [8] See Supplemental Material at <http://link.aps.org/supplemental/10.1103/PhysRevLett.109.205503> for details.  
 [9] P. F. McMillan, M. Wilson, D. Daisenberger, and D. Machon, *Nature Mater.* **4**, 680 (2005).  
 [10] D. Daisenberger, M. Wilson, P. F. McMillan, R. Quesada Cabrera, M. C. Wilding, and D. Machon, *Phys. Rev. B* **75**, 224118 (2007).  
 [11] D. Daisenberger, T. Deschamps, B. Champagnon, M. Mezouar, R. Quesada Cabrera, M. Wilson, and P. F. McMillan, *J. Phys. Chem. B* **115**, 14246 (2011).  
 [12] S. Sorella, M. Casula, L. Spanu, and A. Dal Corso, *Phys. Rev. B* **83**, 075119 (2011).  
 [13] R. Maezono, N. D. Drummond, A. Ma, and R. J. Needs, *Phys. Rev. B* **82**, 184108 (2010).  
 [14] B. Welber, C. K. Kim, M. Cardona, and S. Rodriguez, *Solid State Commun.* **17**, 1021 (1975).  
 [15] D. Keating, A. Nunes, B. Batterman, and J. Hastings, *Phys. Rev. B* **4**, 2472 (1971).  
 [16] J. B. Roberto, B. W. Batterman, and D. T. Keating, *Phys. Rev. B* **9**, 2590 (1974).  
 [17] D. R. Yoder-Short, R. Colella, and B. A. Weinstein, *Phys. Rev. Lett.* **49**, 1438 (1982).  
 [18] K. Fuchizaki and Y. Yamada, *Phys. Rev. B* **40**, 4740 (1989).  
 [19] M. B. Salamon, M. E. Meichle, and C. M. Wayman, *Phys. Rev. B* **31**, 7306 (1985).  
 [20] S. M. Shapiro, Y. Noda, Y. Fujii, and Y. Yamada, *Phys. Rev. B* **30**, 4314 (1984).  
 [21] T. Shigenari, E. Kojima, Y. Ino, and K. Abe, *Phys. Rev. Lett.* **66**, 2112 (1991).  
 [22] Y. Kuroiwa, H. Muramoto, T. Shobu, H. Tokumichi, Y. Noda, and Y. Yamada, *J. Phys. Soc. Jpn.* **64**, 3798 (1995).  
 [23] H. Katzke, U. Bismayer, and P. Tolédano, *Phys. Rev. B* **73**, 134105 (2006).  
 [24] A. S. Mikhaylushkin, U. Häussermann, B. Johansson, and S. I. Simak, *Phys. Rev. Lett.* **92**, 195501 (2004).